Global Point Source CO_2 Emissions Monitoring Based on Hyperspectral Remote Sensing Imagery

Huayi Wang [1,2], Ge Han [1,2,*], Zhipeng Pei [1,2]

[1] Hubei Key Laboratory of Quantitative Remote Sensing of Land and Atmosphere, School of Remote Sensing and Information Engineering, Wuhan University, Wuhan, Hubei, China; – huayiwang818@whu.edu.cn
[2] Perception and Effectiveness Assessment for Carbon-neutrality Efforts, Engineering Research Center of Ministry of Education, Institute for Carbon Neutrality, Wuhan University, Wuhan, Hubei, China – udhan@whu.edu.cn

Keywords: Hyperspectral Remote Sensing, CO_2 point source, Emission Monitoring, Matched Filter, Integrated Mass Enhancement

Abstract
This study presents a hyperspectral remote sensing approach for monitoring global CO_2 point source emissions using China’s GF5 and ZY1 satellites. By applying the matched filter method in the 1.6 μm and 2.0 μm absorption band and the Integrated Mass Enhancement (IME) technique, this study successfully detects and quantifies emissions from multiple facilities within a single scene—demonstrated in a high-density industrial cluster in Xinjiang. Results show current systems can detect power plants with annual emissions above 2.90 $MtCO_2$, covering 6.74 $GtCO_2$/year globally across eight sectors. While power and chemical sectors are well captured, cement and petrochemical emissions remain poorly detected, highlighting the need for improved sensitivity to low-intensity sources.

1. Introduction

International climate negotiations under the United Nations Framework Convention on Climate Change, particularly the annual Conference of the Parties, have progressively elevated the demand for transparent, independent, and high resolution emission monitoring(Cusworth et al., 2024; Duren et al., 2019; Han, Pei, et al., 2024; Thorpe et al., 2023). Since the Paris Agreement was adopted at COP21 in 2015 and reinforced by the Global Stocktake at COP28 in 2023, countries are under growing pressure to move from pledges to verifiable, sector specific mitigation actions (Li et al., 2024). In this context, satellite remote sensing has become indispensable for providing objective, near real time data to support national reporting, cross check inventories, and enhance accountability in global climate governance.

Recent breakthroughs in spaceborne imaging spectroscopy have enabled routine detection of methane point sources at approximately 30 m resolution across oil and gas, waste, and coal sectors (Foote et al., 2021; Foote et al., 2020; Han, Huang, et al., 2024; Han, Pei, et al., 2024; Han et al., 2025; Kim et al., 2025; Li et al., 2026; Pei et al., 2023; Roger et al., 2025; Roger et al., 2024). By contrast, carbon dioxide monitoring using similar hyperspectral approaches remains limited. While early demonstrations with OCO-2 and EMIT have successfully identified carbon dioxide plumes from large power plants (Cusworth et al., 2023; Nassar et al., 2021; Thorpe et al., 2023), these efforts have largely focused on a single satellite sensor or a limited set of facilities. Applications to other major emitting industries, such as petrochemicals, cement, and steel, have not yet been systematically developed. Moreover, the potential of emerging wide swath hyperspectral missions, including China’s GF5 and ZY1 series, for multi source, facility scale carbon dioxide monitoring remains underexplored. Bridging this gap is critical to delivering the facility level emission data required by evolving transparency frameworks under the Paris Agreement and future COP decisions.

The methodological foundation for gas plume detection from imaging spectroscopy is well established(Ayasse et al., 2019; Cusworth et al., 2021; Foote et al., 2020; Guanter et al., 2021; Irakulis-Loitxate et al., 2021; Nelson et al., 2024; Pei et al., 2023). The matched filter algorithm has been widely used for retrieving concentration enhancements of trace gases, including methane and carbon dioxide, by exploiting their characteristic absorption features (Foote et al., 2021; Pei et al., 2023). Similarly, the Integrated Mass Enhancement method, originally developed for airborne data, provides a mass balance approach to convert column enhancements into emission rates (Cusworth et al., 2023). Although these techniques are not new, their application to carbon dioxide point source monitoring using Chinese wide swath hyperspectral data, and more importantly their systematic validation across diverse industrial sectors and geographic conditions, has not been comprehensively addressed in the literature. Prior studies have largely focused on single sensors or specific source types, leaving a gap in understanding the operational capabilities and limitations of current hyperspectral systems for global scale carbon dioxide point source monitoring.

In this study, we aim to fill this gap by systematically applying and evaluating the matched filter and Integrated Mass Enhancement methods for carbon dioxide point source monitoring using GF5 and ZY1 hyperspectral imagery. Specifically, we (1) demonstrate the capability of wide swath hyperspectral data to simultaneously detect and quantify multiple industrial carbon dioxide sources within a single scene, (2) establish a detection threshold linking satellite based detectability to annual emission rates, and (3) assess the global monitoring potential of current hyperspectral systems across eight industrial sectors. By leveraging the wide swath advantage of Chinese hyperspectral satellites, we further explore their potential for facility level emission attribution in complex industrial zones, addressing the urgent need for independent carbon dioxide verification under the Paris Agreement. A previous version of some methodological descriptions and case studies appeared in our preprint (Wang et al., 2025); the present work has been significantly rewritten and extended. The remainder of this paper is organized as follows. Section 2 describes the satellite data and retrieval methodology. Section 3 presents experimental results and detection threshold analysis. Section 4 discusses the implications, limitations, and future directions. Section 5 concludes the study.

* Corresponding author

2. Data and Method

2.1 Hyperspectral Data

Table 1 presents the detailed parameters of multiple hyperspectral satellites currently available for greenhouse gas emission retrieval. The primary data sources used in this study are the GF5 and ZY1 satellite series. The GF5 series consists of two satellites, GF5A and GF5B, while the ZY1 series comprises ZY1E and ZY1F. Both the GF5 and ZY1 series achieve a spatial resolution of 30 m, which is comparable to that of international satellites such as PRISMA and EnMAP. The spectral resolution of the ZY1 satellite is 16 nm, which is relatively low among this class of satellites, whereas the GF5 satellite offers a spectral resolution of approximately 8 nm, approaching the performance of the EMIT satellite, which has a spectral resolution of 7.4 nm. All satellites provide shortwave infrared data covering the spectral range of 1000–2500 nm, and visible and near-infrared data covering 400–1000 nm. Notably, the EMIT satellite does not explicitly separate VNIR and SWIR data; instead, it presents the data as a continuous spectral band.

Satellite	GF5	ZY1	EMIT	PRISMA	EnMAP
VNIR Channels	150	76	285	66	88
SWIR Channels	180	90		173	154
Spatial Resolution (m)	30	30	60	30	30
Spectral Resolution (nm)	8	16	7.4	12	10

Table 1. Comparison of the parameter of satellite sensors

2.2 Calculation of Gas Spectral Feature

The CO_2 spectral signature vector t used in this study was obtained through simulations using the MODTRAN radiative transfer model. Based on the spectral response functions of each satellite sensor, the theoretical spectral absorption features of CO_2 in the absorption bands near 1.6 μm and 2.0 μm were calculated. To minimize potential interference from other trace gases such as water vapor (H_2O) and methane (CH_4), the simulations were conducted under standard atmospheric conditions. The sensitive channels of CH_4 and H_2O were first analyzed. Subsequently, only the differentiated spectral features of CO_2 absorption channels within the ranges of 1560–1630 nm and 1960–2080 nm were extracted for subsequent matched filter retrieval. This processing strategy effectively reduces cross interference from non target gases in the retrieval of CO_2 concentration enhancements.

2.3 Preprocess and Postprocess

The preprocessing workflow begins with the removal of cloud contaminated imagery, primarily excluding scenes where emission facilities are completely obscured by thick clouds. For partially cloudy scenes, a standard cloud masking strategy is applied to remove cloud covered areas before subsequent background spectral statistics and concentration enhancement retrieval. Radiometric calibration is performed after cloud masking, with the primary objective of converting the raw digital number (DN) values of the imagery into physically meaningful radiance values.

The postprocessing workflow primarily involves geometric correction. This is accomplished using the rational polynomial coefficient (RPC) files provided with the AHSI Level 1 data to perform polynomial correction on the imagery, thereby eliminating geometric distortions and ensuring accurate spatial correspondence between the retrieval results and actual geographic locations. The final output imagery products can be used for subsequent CO_2 concentration enhancement retrieval and emission rate calculation.

2.4 Matched Filter

Matched filter is a statistical method based on data, which is used for signal detection and quantification in hyperspectral images. Matched filter is able to accurately extract the enhanced signals of interest for CO_2 or methane gas concentrations from noisy backgrounds. CO_2 concentration enhancements are retrieved using the matched filter method in the 1.6 μm and 2.0 μm absorption band.

The matched filter formula is as follows (Pei et al., 2023):

$$\hat{\Delta c} = \frac{\boldsymbol{t}^T \boldsymbol{\Sigma}^{-1}(\boldsymbol{x_m}-\boldsymbol{\mu})}{\boldsymbol{t}^T \boldsymbol{\Sigma}^{-1} \boldsymbol{t}}, \quad (1)$$

where $\hat{\Delta c}$ = the concentration enhancement of gas
$\boldsymbol{x_m}$ = observed spectral vector
$\boldsymbol{\mu}$ = the mean spectral vector of the image
$\boldsymbol{t}$ = the spectral feature of gas
$\boldsymbol{\Sigma}$ = the covariance of the measured spectrum

2.5 Integrated Mass Enhancement

Based on the CO_2 column concentration enhancement field derived from matched filtering, we subsequently quantified emission rates using the Integrated Mass Enhancement (IME) method, which incorporates local wind and atmospheric parameters. Specifically, both the vertical mass of atmosphere (VMA) and wind speed data were sourced from the ERA5 reanalysis dataset.

The IME calculation formula is as follows:

$$IME = \sum_{i=1}^{n} (VMA \cdot \frac{M_{CO_2}}{M_{dry}} \cdot A \cdot \hat{\Delta c}(i)), \quad (2)$$

where VMA = vertical mass of atmosphere
M_{CO_2} = molar mass of carbon dioxide
M_{dry} = average molar mass of dry air
A = actual area of the cell (m^2)

The emission rate formula is as follows:

$$Q = IME \cdot \frac{U_{eff}}{L}, \quad (3)$$

where Q = facility emission rate (ton/h)
U_{eff} = effective wind speed (m/s)
L = plume length (m)

3. Results and Discussions

3.1 Single-Scene Multi-Source Observation Case

Zhundong, Xinjiang, China, is a typical coal production hub, where multiple coal-fired power plants and coal chemical enterprises are highly concentrated to maximize the efficiency of coal resource utilization. For emission scenarios such as this, OCO-2/3 can only treat all sources as a single aggregate, estimating total emissions for the entire industrial park. However, these emission sources are not governed by a single corporate entity. This situation is common in energy-driven regional economies, highlighting the pressing need to develop high-

resolution CO_2 plume-based point-source monitoring for improved emission accountability.

Due to the limitations in spatial resolution and coverage of early satellite-derived XCO_2 products (e.g., GOSAT, OCO-2/3), emissions from multiple concentrated point sources are often aggregated into a single estimate. In practice, however, industrial parks typically consist of several independent entities, making it necessary to attribute emissions to individual factories or even specific facilities. To address this challenge, we designed and conducted a multi-point-source quantification experiment within a single field of view at an industrial park in Zhundong, Xinjiang, China. The AHSI sensor provides hyperspectral data with a swath width of 60 km, which significantly expands our field of view. In comparison, satellites such as PRISMA and EnMAP have swath widths of only about 30 km, and the coverage area per scene is approximately one-quarter that of AHSI. This broader coverage enables a single AHSI image to simultaneously detect and quantify more point sources, thereby enhancing the large-scale application potential of emission quantification methods.

id	latitude	longitude	emission	wind_speed
A	44.8972	89.2461	271±56t/h	3.06m/s
B	44.8544	89.1972	1507±215t/h	3.47m/s
C	44.8408	89.1946	2029±274t/h	3.62m/s
D	44.8065	89.1946	734±109t/h	3.62m/s
E	44.7889	89.1907	499±79t/h	3.62m/s
F	44.7979	89.1472	558±87t/h	3.62m/s
G	44.6972	89.1169	538±90t/h	3.13m/s
H	44.6843	89.1167	683±111t/h	3.13m/s

Table 2. Multi-point Source Quantification Results from GF5B Satellite over Xinjiang, China, on July 22, 2022

Quantifying multiple point sources simultaneously within a single image facilitates a more robust comparison of the relative emission intensities among sources. This is because meteorological parameters such as temperature, water vapor, and wind speed are essentially consistent across the same image, effectively controlling for confounding variables. Previous analysis(Han et al., 2026) shows that the main source of uncertainty in emission intensity is wind speed variability. Nevertheless, over local distances (approximately 10 km), wind speeds tend to be relatively uniform. This means that variations in plume intensities within a single image largely reflect characteristics of the retrieval method itself rather than differences in wind speed. On this basis, the relative emission intensities of individual vents can be determined with high precision. For example, if the emission intensity of a known source, such as a government-regulated facility with regularly inventoried emissions, is available, the emissions of nearby unregulated sources can be estimated proportionally using single-field multi-point-source inversion, thereby achieving more accurate emission accounting.

As shown in Figure 1, we identified and quantified eight emission sources within an area of less than 30 km², with intensities ranging from 271 t/h to 2029 t/h. Among these, sources B through F are even more densely concentrated, lying within a 3 km × 10 km region. Through visual interpretation of high-resolution optical imagery and comparative analysis with map data, we identified these sources as five coal-fired power plants and three chemical plants. (The corresponding quantitative results are listed in Table 2.)

The above results demonstrate that the single-field multi-point-source inversion method based on AHSI wide-swath hyperspectral data can simultaneously capture multiple densely distributed emission sources in a single overpass and effectively distinguish emission differences among various facilities. This verifies the feasibility and reliability of the method for fine-grained emission attribution in complex industrial park scenarios, and provides direct data support for subsequent cross-enterprise, cross-facility emission accounting using relative intensity comparisons.

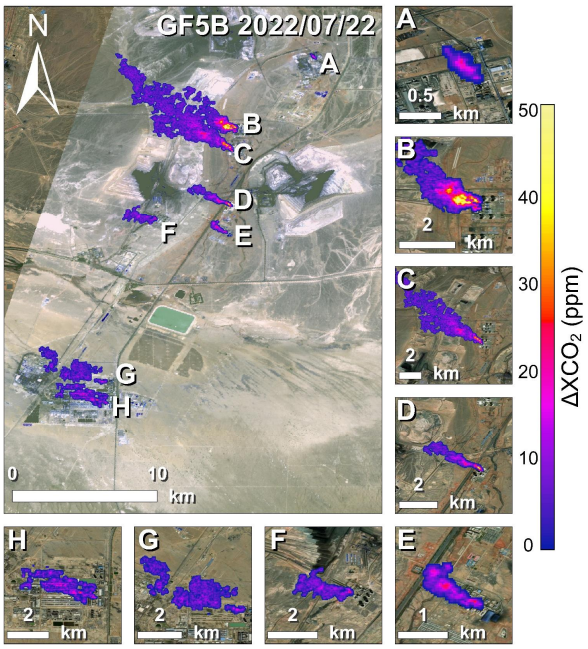

Figure 1. Hyperspectral satellite observations of multiple point sources in Xinjiang, China.

3.2 Detection Threshold Relationship between Satellite Detectability and Annual Emissions

To further quantify detection capabilities, we established a statistical relationship between detection probability and annual emissions based on the $CoCO_2$ dataset(Gon, 2023), integrating real satellite observations and hourly plant-level emission estimates (Figure 2). The analysis indicates that power plants with annual emissions exceeding 2.90 Mt have a 50% probability of being detected by current satellite systems. This threshold serves as a practical benchmark for planning future hyperspectral satellite missions and prioritizing key emission sources.

As illustrated in Figure 2, we fitted the detection probability curve using a cumulative distribution function modeled as an error function:

$$F(x|\mu,\sigma) = \frac{1}{2}[1 + \mathrm{erf}\,(\frac{x-\mu}{\sigma\sqrt{2}})], \quad (4)$$

where $\mu = 2.90\times10^6$ (tCO_2/yr);
$\sigma = 4.80\times10^5$ (tCO_2/yr).

The curve characteristics reveal a typical S-shaped growth trend in detection probability. When annual emissions are below 2 Mt, the detection probability approaches zero. Within the 2 to 4 Mt range, the probability rises rapidly, indicating this range represents a sensitive transition zone for satellite detection

capability. Once emissions exceed 5 Mt, the detection probability approaches 100%, and the 95% confidence interval narrows significantly, demonstrating high reliability in detecting large emission sources.

This statistical relationship reveals the detection performance boundaries of current hyperspectral satellite systems. For large coal-fired power plants with annual emissions exceeding 4 Mt, satellite monitoring can achieve stable and continuous tracking. For medium-sized emission sources in the 2 to 3 Mt range, the detection success rate is approximately 30%, necessitating multi-temporal observations or data fusion strategies to improve detection rates. For small facilities with emissions below 2Mt, the detection capability of existing technology remains limited. This imposes higher requirements on the design of next-generation satellite sensors, including improving signal-to-noise ratios, optimizing spectral resolution, and enhancing temporal coverage frequency.

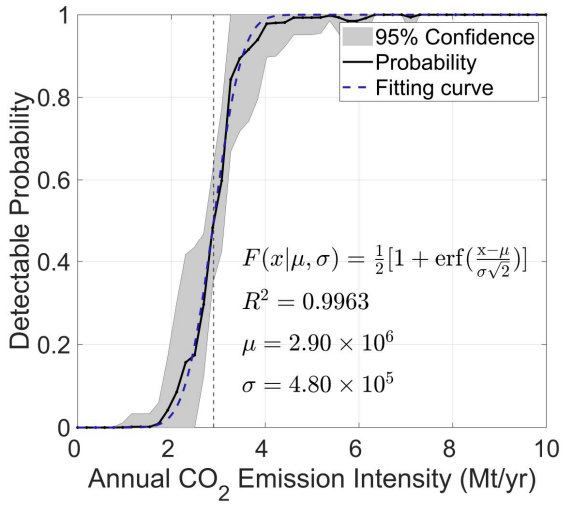

Figure 2. Detection probability and annual emission intensity.

3.3 Assessment of Global Monitoring Potential across Industrial Sectors

In current satellite-based CO_2 point source monitoring, thermal power plants receive the most attention because they release emissions at high intensities and occupy well-defined locations. For these facilities, emission levels can already be quantified reliably using methods such as continuous emission monitoring systems or coal ash analysis, and remote sensing offers a cost-effective, transparent way to independently verify reported data. By contrast, sectors like cement and steel production still lack widely accepted and trustworthy methodologies for CO_2 monitoring. This shortcoming poses a serious obstacle to global carbon accounting, as these industries produce substantial emissions that often remain poorly quantified. Here we show that our proposed method can quantify CO_2 point source emissions across multiple industrial sectors, thereby providing a fresh approach to monitoring and verification beyond the power generation industry. We argue that this remote sensing innovation can deliver unprecedented support for establishing rigorous monitoring, reporting, and verification (MRV) practices in the steel and cement sectors, thus filling a critical gap in current CO_2 MRV systems.

Figure 3 presents quantification results from the energy, steel, cement, and petrochemical sectors. The key finding is that satellite based remote sensing works effectively for point sources in all these industries, provided their emission intensities lie above the detection threshold. This result confirms the wide applicability of our method and suggests strong potential for large scale deployment in industrial carbon monitoring. To better understand how well existing satellites can cover emissions worldwide, we combined our detection limits with the Climate TRACE database (*Climate Trace Global Emission*, 2025). The analysis covered eight industrial categories: electricity generation, oil and gas production, oil and gas refining, iron and steel production, cement production, chemical manufacturing, aluminum production, and petrochemical steam cracking. Across these categories, 5,449 emission sources were examined. Of these, 756 sources exceeded the detection limits of satellite based remote sensing, together releasing 6,742.7 megatons of CO_2 per year. If considered as a single emitter, this group would rank second globally, outpacing the combined emissions of the 27 European Union member states and India, or the total emissions of the United States and Russia.

Nevertheless, emission intensities vary considerably from one industry to another. As shown in Figure 3, roughly 66% of CO_2 emissions from power generation can be captured by the proposed methods, whereas for the cement industry the proportion falls to just 10%. Such differences reveal the difficulty of detecting emission sources with lower intensities or spatially diffuse plumes. They also underline the need for further improvements in high resolution CO_2 remote sensing to enhance monitoring capabilities across all major emitting industries.

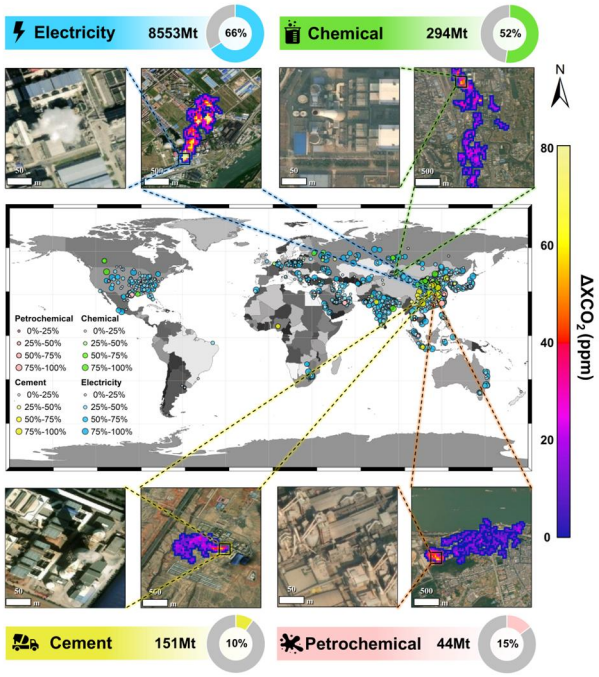

Figure 3. Point source carbon monitoring applications for various industries.

4. Discussion

This study systematically validates the application potential of domestic wide-swath hyperspectral satellites (GF5/ZY1) for global CO_2 point source monitoring. Although the matched filter and IME methods are not novel, this study represents the first systematic application of these techniques to Chinese hyperspectral satellite data with large-scale validation across multiple industrial sectors, filling a gap in the assessment of

wide-swath hyperspectral satellite capabilities for facility-level CO_2 monitoring.

4.1 Method Advantages and Application Value

The core advantage of this study lies in fully leveraging the 60-km swath width of GF5 and ZY1 satellites. Compared to international satellites such as PRISMA and EnMAP with approximately 30-km swath widths, our approach can simultaneously detect more point sources within a single scene. In the Zhundong, Xinjiang case, we successfully identified and quantified more than eight emission sources (ranging from 271 to 2029 t/h) within an area of less than 30 km², significantly improving monitoring efficiency in dense industrial regions. Detection threshold analysis indicates that the current system can reliably detect power plants with annual emissions exceeding 2.90 $MtCO_2$. At the global scale, this capability can cover approximately 6.74 $GtCO_2$/year across eight industrial sectors, with approximately 66% of emissions from the power sector being quantifiable, providing important technical support for independent verification under the Paris Agreement framework.

4.2 Uncertainties and Limitations

The current method still faces several major sources of uncertainty: (1) Aerosol interference: Under high AOD conditions, the relative error in CO_2 concentration enhancement is approximately 15–25%, necessitating integration with multi-spectral aerosol products or development of joint retrieval algorithms in the future; (2) Wind speed data errors: ERA5 wind speed errors are the primary source of uncertainty in emission rate estimates, which could be mitigated by interpolating multi-source reanalysis data; (3) Background selection bias: Obtaining "clean" background pixels in highly industrialized regions is challenging, potentially leading to underestimation of concentration enhancements, making accurate background pixel selection a prerequisite for precise quantification; (4) Limited detection of low-intensity sources: The detection probability for facilities with annual emissions below 2 $MtCO_2$ approaches zero, with only 10% of emission sources in the cement sector being detectable, highlighting an urgent need to improve sensor signal-to-noise ratios and spectral resolution.

4.3 Policy Implications and Future Directions

This study has important implications for carbon verification systems: satellite remote sensing can significantly reduce per-enterprise verification costs compared to traditional methods while maintaining monitoring accuracy comparable to CEMS; its high transparency helps prevent data falsification and enhances carbon market credibility.

Precise emissions quantification at the factory or facility level can significantly enhance government oversight of major polluters. Hubei Province, for example, allocates over 10 million RMB annually for carbon audits across 500 enterprises, averaging only 20,000 RMB per firm. Such fiscal constraints are common in developing nations, leading to widespread skepticism about the accuracy of these audits.

To resolve this dilemma, satellite remote sensing technology can be deployed to monitor key emitters. This approach could drastically cut auditing costs while maintaining an accuracy comparable to Continuous Emissions Monitoring Systems (CEMS). Furthermore, the high transparency of satellite data bolsters stakeholder confidence in emission reports, thereby strengthening the foundation of trust in carbon accounting and compliance frameworks.

Future research should focus on: (1) integrating multi-source satellite and ground-based data for multi-scale validation; (2) developing global operational monitoring systems to support the Paris Agreement Global Stocktake. Although current technologies still have limitations, the advantages of hyperspectral remote sensing for facility-level emission attribution have been validated, with the potential to drive a paradigm shift in carbon monitoring from "regional aggregate estimation" toward "facility-level precise attribution."

5. Conclusions

This study validates the potential of domestic hyperspectral satellites for global CO_2 point source emission monitoring. Through a synergistic framework combining matched filtering and IME-based quantification, we achieved refined, facility-level emission estimates within industrial clusters. Our results indicate that the current technical system possesses robust monitoring capability for medium-to-high intensity emission sources (>2.90 $MtCO_2$/year), providing independent and transparent remote sensing evidence for emission verification in key sectors such as power generation and chemicals. Nevertheless, technical challenges persist in detecting low-intensity or process-complex sources from industries like cement and petrochemicals. Future efforts should focus on optimizing spectral retrieval algorithms and integrating multi-source meteorological data to improve weak-signal extraction performance. With continuous observations from next-generation satellites such as GF5B and ZY1E, along with iterative algorithm improvements, hyperspectral remote sensing is poised to become a critical technical pillar for the Global Stocktake and compliance monitoring under the Paris Agreement. This advancement facilitates a paradigm shift in carbon emission monitoring, moving from regional aggregate estimation toward facility-level precise attribution, and contributes a Chinese solution to building a fair, efficient, and verifiable international carbon governance framework.

References

Ayasse, A. K., Dennison, P. E., Foote, M., Thorpe, A. K., Joshi, S., Green, R. O., Duren, R. M., Thompson, D. R., & Roberts, D. A. (2019). Methane Mapping with Future Satellite Imaging Spectrometers. *Remote Sensing*, *11*(24). https://doi.org/10.3390/rs11243054

Climate Trace Global Emission. (2025). https://climatetrace.org/

Cusworth, D. H., Duren, R. M., Ayasse, A. K., Jiorle, R., Howell, K., Aubrey, A., Green, R. O., Eastwood, M. L., Chapman, J. W., Thorpe, A. K., Heckler, J., Asner, G. P., Smith, M. L., Thoma, E., Krause, M. J., Heins, D., & Thorneloe, S. (2024). Quantifying methane emissions from United States landfills. *Science*, *383*(6690), 1499-1504. https://doi.org/10.1126/science.adi7735

Cusworth, D. H., Duren, R. M., Thorpe, A. K., Eastwood, M. L., Green, R. O., Dennison, P. E., Frankenberg, C., Heckler, J. W., Asner, G. P., & Miller, C. E. (2021). Quantifying Global Power Plant Carbon Dioxide Emissions With Imaging Spectroscopy. *Agu Advances*, *2*(2).

Cusworth, D. H., Thorpe, A. K., Miller, C. E., Ayasse, A. K., Jiorle, R., Duren, R. M., Nassar, R., Mastrogiacomo, J. P., & Nelson, R. R. (2023). Two years of satellite-

based carbon dioxide emission quantification at the world's largest coal-fired power plants. *Atmospheric Chemistry and Physics*, *23*(22), 14577-14591.

Duren, R. M., Thorpe, A. K., Foster, K. T., Rafiq, T., Hopkins, F. M., Yadav, V., Bue, B. D., Thompson, D. R., Conley, S., Colombi, N. K., Frankenberg, C., McCubbin, I. B., Eastwood, M. L., Falk, M., Herner, J. D., Croes, B. E., Green, R. O., & Miller, C. E. (2019). California's methane super-emitters [Article]. *Nature*, *575*(7781), 180-184. https://doi.org/10.1038/s41586-019-1720-3

Foote, M. D., Dennison, P. E., Sullivan, P. R., O'Neill, K. B., Thorpe, A. K., Thompson, D. R., Cusworth, D. H., Duren, R., & Joshi, S. C. (2021). Impact of scene-specific enhancement spectra on matched filter greenhouse gas retrievals from imaging spectroscopy. *Remote Sensing of Environment*, *264*. https://doi.org/10.1016/j.rse.2021.112574

Foote, M. D., Dennison, P. E., Thorpe, A. K., Thompson, D. R., Jongaramrungruang, S., Frankenberg, C., & Joshi, S. C. (2020). Fast and Accurate Retrieval of Methane Concentration From Imaging Spectrometer Data Using Sparsity Prior. *Ieee Transactions on Geoscience and Remote Sensing*, *58*(9), 6480-6492. https://doi.org/10.1109/Tgrs.2020.2976888

Gon, M. G. E. T. J. P. G.-P. D. D. v. d. (2023). *CoCO2 global emission point source database - v2.0*

Guanter, L., Irakulis-Loitxate, I., Gorroño, J., Sánchez-García, E., Cusworth, D. H., Varon, D. J., Cogliati, S., & Colombo, R. (2021). Mapping methane point emissions with the PRISMA spaceborne imaging spectrometer. *Remote Sensing of Environment*, *265*.

Han, G., Huang, Y. Y., Shi, T. Q., Zhang, H. Y., Li, S. W., Zhang, H. W., Chen, W. B., Liu, J. Q., & Gong, W. (2024). Quantifying CO2 emissions of power plants with Aerosols and Carbon Dioxide Lidar onboard DQ-1. *Remote Sensing of Environment*, *313*. https://doi.org/10.1016/j.rse.2024.114368

Han, G., Pei, Z. P., Shi, T. Q., Mao, H. Q., Li, S. W., Mao, F. Y., Ma, X., Zhang, X. Y., & Gong, W. (2024). Unveiling Unprecedented Methane Hotspots in China's Leading Coal Production Hub: A Satellite Mapping Revelation. *Geophysical Research Letters*, *51*(10), e2024GL109065. https://doi.org/10.1029/2024GL109065

Han, G., Wang, H., Pei, Z., Mao, H., Ying, J., Li, S., Ma, X., Liu, B., Mao, F., & Gong, W. (2026). Quantifying facility-scale CO2 emissions using spaceborne hyperspectral imageries. *Remote Sensing of Environment*, *342*, 115478. https://doi.org/https://doi.org/10.1016/j.rse.2026.115478

Han, G., Zhang, H., Huang, Y., Chen, W., Mao, H., Zhang, X., Ma, X., Li, S., Zhang, H., Liu, J., Mao, F., & Gong, W. (2025). First global XCO2 observations from spaceborne lidar: methodology and initial result. *Remote Sensing of Environment*, *330*, 114954. https://doi.org/https://doi.org/10.1016/j.rse.2025.114954

Irakulis-Loitxate, I., Guanter, L., Liu, Y. N., Varon, D. J., Maasakkers, J. D., Zhang, Y., Chulakadabba, A., Wofsy, S. C., Thorpe, A. K., Duren, R. M., Frankenberg, C., Lyon, D. R., Hmiel, B., Cusworth, D. H., Zhang, Y., Segl, K., Gorrono, J., Sanchez-Garcia, E., Sulprizio, M. P., . . . Jacob, D. J. (2021). Satellite-based survey of extreme methane emissions in the Permian basin. *Science Advances*, *7*(27). https://doi.org/10.1126/sciadv.abf4507

Kim, J., Cusworth, D. H., Ayasse, A. K., Howell, K., O’Neill, K., & Duren, R. M. (2025). Performance of Airborne Imaging Spectrometers for Carbon Dioxide Detection and Emission Quantification. *Journal of Geophysical Research: Atmospheres*, *130*(7), e2024JD042755. https://doi.org/https://doi.org/10.1029/2024JD042755

Li, F., Lin, K., Yan, Y., Bai, S., Huang, Q., Feng, C., Sun, S., Zhao, S., Zhou, W., Zhou, C., Lin, J., Zhang, X., & Zhang, Y. (2026). Comparing the performance of different hyperspectral satellite imaging spectroscopy in mapping methane point-source emissions. *Remote Sensing of Environment*, *334*, 115224. https://doi.org/https://doi.org/10.1016/j.rse.2025.115224

Li, S. P., Meng, J., Hubacek, K., Eskander, S. M. S. U., Li, Y., Chen, P. P., & Guan, D. B. (2024). Revisiting Copenhagen climate mitigation targets. *Nature Climate Change*, *14*(5). https://doi.org/10.1038/s41558-024-01977-5

Nassar, R., Mastrogiacomo, J. P., Bateman-Hemphill, W., McCracken, C., MacDonald, C. G., Hill, T., O'Dell, C. W., Kiel, M., & Crisp, D. (2021). Advances in quantifying power plant CO2 emissions with OCO-2. *Remote Sensing of Environment*, *264*. https://doi.org/10.1016/j.rse.2021.112579

Nelson, R. R., Cusworth, D. H., Thorpe, A. K., Kim, J., Elder, C. D., Nassar, R., & Mastrogiacomo, J.-P. (2024). Comparing Point Source CO2 Emission Rate Estimates From Near-Simultaneous OCO-3 and EMIT Observations. *Geophysical Research Letters*, *51*(23), e2024GL113002. https://doi.org/https://doi.org/10.1029/2024GL113002

Pei, Z. P., Han, G., Mao, H. Q., Chen, C. H., Shi, T. Q., Yang, K. Y., Ma, X., & Gong, W. (2023). Improving quantification of methane point source emissions from imaging spectroscopy [Article]. *Remote Sensing of Environment*, *295*, Article 113652.

Roger, J., Guanter, L., & Gorroño, J. (2025). Assessing the Detection of Methane Plumes in Offshore Areas Using High-Resolution Imaging Spectrometers. *Atmos. Meas. Tech.*, *18*(20), 5545-5567. https://doi.org/10.5194/amt-18-5545-2025

Roger, J., Guanter, L., Gorroño, J., & Irakulis-Loitxate, I. (2024). Exploiting the entire near-infrared spectral range to improve the detection of methane plumes with high-resolution imaging spectrometers. *Atmospheric Measurement Techniques*, *17*(4), 1333-1346. https://doi.org/10.5194/amt-17-1333-2024

Thorpe, A. K., Green, R. O., Thompson, D. R., Brodrick, P. G., Chapman, J. W., Elder, C. D., Irakulis-Loitxate, I., Cusworth, D. H., Ayasse, A. K., Duren, R. M., Frankenberg, C., Guanter, L., Worden, J. R., Dennison, P. E., Roberts, D. A., Chadwick, K. D., Eastwood, M. L., Fahlen, J. E., & Miller, C. E. (2023). Attribution of individual methane and carbon dioxide emission sources using EMIT observations from space. *Science Advances*, *9*(46), eadh2391.

Wang, H., Ge, H., Pei, Z., Mao, H., Ying, J., Li, S., Ma, X., Liu, B., Mao, F., & Gong, W. (2025). *Towards global carbon transparency: Spaceborne imaging spectroscopy enables precise CO2 emission quantification at facility scale*. https://doi.org/10.21203/rs.3.rs-5913782/v1